## $^{77}$Ni $\beta^-$ decay (158.9 ms) 2017Sa32

| History | | | |
|---|---|---|---|
| Type | Author | Citation | Literature Cutoff Date |
| Full Evaluation | Balraj Singh | ENSDF | 30-Sep-2020 |

Parent: $^{77}$Ni: E=0; $J^\pi$=(9/2$^+$); $T_{1/2}$=158.9 ms *42*; Q($\beta^-$)=12063 *SY*; %$\beta^-$ decay=100.0

$^{77}$Ni-$J^\pi$: From systematics, dominated by an odd neutron hole in the $1g_{9/2}$ orbital in the shell-model calculations (2017Sa32).

$^{77}$Ni-$T_{1/2}$: From $^{77}$Ni Adopted Levels, where the value is from 2014Xu07.

$^{77}$Ni-Q($\beta^-$): 12063 *500* (from mass excess for $^{77}$Ni from 2017Wa10, and measured mass excess for $^{77}$Cu from 2017We16. Other: 11820 *520* (syst, 2017Wa10).

$^{77}$Ni-%$\beta^-$ decay: %$\beta^-$n=24 *16* (2014XuZZ), 30 *24* (2010Ho12) for the decay of $^{77}$Ni. Note also that 22.4 *16* units of absolute $\gamma$ intensity are unplaced in the level scheme.

2017Sa32: $^{77}$Ni isotope produced in $^{9}$Be($^{238}$U,F) reaction at E=345 MeV/nucleon. Nuclei of $^{77}$Ni were identified by atomic number (Z) and mass/charge (A/Q) ratio by time-of-flight (tof), magnetic rigidity (B$\rho$) and energy loss $\Delta$E using the BigRIPS fragment separator and ZeroDegree spectrometer. Particles (the implanted ions, $\beta$ rays from the decay of $^{77}$Ni and conversion electrons) were detected by WAS3ABi silicon detector array, and $\gamma$ radiation by EURICA array of 84 HPGe detectors in 12 clusters. Measured ($^{77}$Ni ions)$\gamma$-correlated events, E$\gamma$, I$\gamma$, $\gamma\gamma$-coin. Deduced levels, $J^\pi$, $\beta$ feedings, log *ft* values. Comparison with shell-model calculations. Conference report 2016Sa07 is from the same group.

Includes revised data Table of $\gamma$-ray intensities and comments received from F.L. Bello Garrote and E. Sahin, authors of 2017Sa32 on June 5, 2020.

### $^{77}$Cu Levels

| E(level)[†] | $J^\pi$[‡] | $T_{1/2}$ | Comments |
|---|---|---|---|
| 0 | 5/2$^-$ | 469.8 ms *20* | $J^\pi$,$T_{1/2}$: from $^{77}$Cu Adopted Levels. |
| 293 *1* | (3/2$^-$) | | |
| 946 *1* | (9/2$^-$) | | |
| 1154 *1* | (7/2$^-$) | | |
| 1776 *1* | (13/2$^-$) | | |
| 1955 *1* | (11/2$^-$) | | |
| 2068 *1* | (7/2$^-$) | | E(level): the level is tentative in 2017Sa32, but based on $^{9}$Be($^{78}$Zn,p$\gamma$) data in 2018Va08, the level is certain from the observation of a strong 2068$\gamma$. |
| 2605 *2* | (11/2,13/2$^-$) | | |
| 2695? *2* | (7/2$^-$) | | E(level),$J^\pi$: tentative level proposed in revised data Table and comments received, June 5, 2020 from the authors of 2017Sa32. |
| 2869 *2* | (11/2,13/2$^-$) | | |
| 2909 *2* | (9/2,11/2$^-$) | | |
| 3412 *2* | (9/2,11/2$^-$) | | |
| 3954 *2* | (7/2,9/2,11/2$^-$) | | |
| 5958+x | | | E(level): level introduced by compiler to account for population of neutron-unbound levels, as suggested by %$\beta^-$n values measured by 2010Ho10 and 2014XuZZ x<6105 *500* from Q($\beta^-$)-S(n)($^{77}$Cu), where Q($\beta^-$)=12063 *500* and S(n)=5958.1 *71* (2017Wa10 and mass measurement by 2017We16). |

[†] Deduced from least-squares fit to E$\gamma$ data.

[‡] As assigned by 2017Sa32 in their level-scheme Fig. 3, based partly on shell-model calculations. The ground-state spin of 5/2 is measured by 2011Ko36.

## $^{77}$Ni $\beta^-$ decay (158.9 ms) 2017Sa32 (continued)

### $\beta^-$ radiations

| E(decay) | E(level) | I$\beta^-$[†][#] | Log $ft$[‡] | Comments |
|---|---|---|---|---|
| (3052[&] *SY*) | 5958+x | 26 *16* | | I$\beta^-$: from %$\beta^-$n=26 *16* of $^{77}$Ni decay (see $^{77}$Ni Adopted Levels). |
| (8109 *SY*) | 3954 | <2.6 | >5.8 | av E$\beta$=3.76×10$^3$ *25*<br>I$\beta^-$: from intensity balance, I$\beta$=2.1 *5*. 2017Sa32 give <2.5. |
| (8651 *SY*) | 3412 | <4.0 | >5.7 | av E$\beta$=4.03×10$^3$ *25*<br>I$\beta^-$: from intensity balance, I$\beta$=3.4 *6*. 2017Sa32 give <3.9. |
| (9154 *SY*) | 2909 | <3.5 | >5.9 | av E$\beta$=4.27×10$^3$ *25*<br>I$\beta^-$: from intensity balance, I$\beta$=3.0 *5*. 2017Sa32 give <3.4. |
| (9194 *SY*) | 2869 | <2.4 | >6.0 | av E$\beta$=4.29×10$^3$ *25*<br>I$\beta^-$: from intensity balance, I$\beta$=1.7 *7*. 2017Sa32 give <2.2. |
| (9368[@] *SY*) | 2695? | <2.2 | >6.1 | av E$\beta$=4.37×10$^3$ *25*<br>I$\beta^-$: from intensity balance, I$\beta$=1.8 *4*. |
| (9458 *SY*) | 2605 | <2.0 | >6.2 | av E$\beta$=4.42×10$^3$ *25*<br>I$\beta^-$: from intensity balance, I$\beta$=1.0 *10*. 2017Sa32 give <1.6. |
| (9995 *SY*) | 2068 | <4.7 | >5.9 | av E$\beta$=4.68×10$^3$ *25*<br>I$\beta^-$: from intensity balance, I$\beta$=4.1 *6*. 2017Sa32 give <4.2. |
| (10108 *SY*) | 1955 | <8.3 | >5.7 | av E$\beta$=4.73×10$^3$ *25*<br>I$\beta^-$: from intensity balance, I$\beta$=7.5 *8*. 2017Sa32 give <8.3. |
| (10287[@] *SY*) | 1776 | <1.7 | >8.8[1u] | av E$\beta$=4.83×10$^3$ *25*<br>I$\beta^-$: from intensity balance, I$\beta$=−0.1 *18*. 2017Sa32 give <3.1. |
| (10909 *SY*) | 1154 | <8.3 | >5.9 | av E$\beta$=5.12×10$^3$ *25*<br>I$\beta^-$: from intensity balance, I$\beta$=7.4 *9*. 2017Sa32 give <6.4. |
| (11117 *SY*) | 946 | <23.3 | >5.4 | av E$\beta$=5.22×10$^3$ *25*<br>I$\beta^-$: from intensity balance, I$\beta$=21.5 *18*. 2017Sa32 give <22.0. |
| (11770[@] *SY*) | 293 | | | av E$\beta$=5.42×10$^3$ *26*<br>I$\beta^-$: from intensity balance, I$\beta$=−1.3 *9*, consistent with no $\beta$ feeding as expected to this level for ΔJ=3, Δπ=yes $\beta$ transition. 2017Sa32 give <1.2. |
| (12063[@] *SY*) | 0 | <10 | >8.5[1u] | av E$\beta$=5.70×10$^3$ *25*<br>I$\beta^-$: assigned by evaluator from log $f^{1u}t$>8.5 for first-forbidden unique $\beta$ transition expected from (9/2$^+$) parent to 5/2$^-$ daughter state. |

[†] Deduced by the evaluator from intensity balances using the data Table for $\gamma$-ray intensity supplied by the authors of 2017Sa32 on June 5, 2020. The values listed in 2017Sa32, in some cases, are slightly different, and are given under comments. Note that in the decay scheme proposed by 2017Sa32, 20% *16* $\beta$ feeding remains unaccounted, and also that 22.4 *16* units of absolute $\gamma$ intensity remains unplaced in the decay scheme.
[‡] Deduced by evaluator using the LOGFT code and Q($\beta^-$)=12063 *500*.
[#] Absolute intensity per 100 decays.
[@] Existence of this branch is questionable.
[&] Estimated for a range of levels.

### $\gamma$($^{77}$Cu)

I$\gamma$ normalization: Absolute $\gamma$-ray intensities are given by 2017Sa32.

| E$_\gamma$ | I$_\gamma$[†][‡] | E$_i$(level) | J$_i^\pi$ | E$_f$ | J$_f^\pi$ | Comments |
|---|---|---|---|---|---|---|
| 179 *1* | 1.8 *4* | 1955 | (11/2$^-$) | 1776 | (13/2$^-$) | |
| [x]256 *1* | 2.7 *4* | | | | | |
| [x]278 *1* | 1.3 *4* | | | | | In coin with 946$\gamma$. |
| 293 *1* | 4.7 *5* | 293 | (3/2$^-$) | 0 | 5/2$^-$ | |

Continued on next page (footnotes at end of table)

## $^{77}$Ni $\beta^-$ decay (158.9 ms) 2017Sa32 (continued)

### $\gamma(^{77}Cu)$ (continued)

| $E_\gamma$ | $I_\gamma$[†‡] | $E_i$(level) | $J_i^\pi$ | $E_f$ | $J_f^\pi$ | Comments |
|---|---|---|---|---|---|---|
| [x]335 *1* | 1.4 *4* | | | | | |
| 543 *1* | 1.4 *4* | 3412 | (9/2,11/2$^-$) | 2869 | (11/2,13/2$^-$) | |
| 801 *1* | 2.2 *4* | 1955 | (11/2$^-$) | 1154 | (7/2$^-$) | |
| 829 *1* | 1.0 *10* | 2605 | (11/2,13/2$^-$) | 1776 | (13/2$^-$) | |
| 830 *1* | 10.8 *12* | 1776 | (13/2$^-$) | 946 | (9/2$^-$) | $E_\gamma$,$I_\gamma$: from revised data Table received from the authors, June 5, 2020. |
| 860 *1* | 4.2 *5* | 1154 | (7/2$^-$) | 293 | (3/2$^-$) | |
| 946 *1* | 37.9 *11* | 946 | (9/2$^-$) | 0 | 5/2$^-$ | |
| 1009 *1* | 3.5 *5* | 1955 | (11/2$^-$) | 946 | (9/2$^-$) | |
| [x]1045 *1* | 0.9 *3* | | | | | |
| 1093 *1* | 3.1 *5* | 2869 | (11/2,13/2$^-$) | 1776 | (13/2$^-$) | |
| 1133 *1* | 3.0 *5* | 2909 | (9/2,11/2$^-$) | 1776 | (13/2$^-$) | |
| 1154 *1* | 5.4 *5* | 1154 | (7/2$^-$) | 0 | 5/2$^-$ | |
| [x]1451 *1* | 2.6 *4* | | | | | In coin with 946$\gamma$. |
| [x]1542 *1* | 0.9 *4* | | | | | |
| [x]1552 *1* | 1.6 *5* | | | | | |
| 1636 *1* | 2.0 *4* | 3412 | (9/2,11/2$^-$) | 1776 | (13/2$^-$) | |
| [x]1708 *1* | 0.8 *4* | | | | | |
| [x]1741 *1* | 2.4 *5* | | | | | |
| 2068 *1* | 4.1 *6* | 2068 | (7/2$^-$) | 0 | 5/2$^-$ | |
| [x]2163 *1* | 0.6 *3* | | | | | |
| [x]2238 *1* | 1.5 *4* | | | | | |
| [x]2313 *1* | 0.7 *3* | | | | | |
| [x]2348 *1* | 0.9 *3* | | | | | |
| 2402[#] *1* | 1.8 *4* | 2695? | (7/2$^-$) | 293 | (3/2$^-$) | Tentative placement suggested from observation of 2402$\gamma$ in coincidence with 293$\gamma$ (Fig. 2 in 2017Sa32), and stated in revised data Table and comments received June 5, 2020 from the authors. |
| [x]2440 *1* | 0.9 *3* | | | | | |
| [x]2521 *1* | 1.6 *4* | | | | | |
| [x]2611 *1* | 1.0 *3* | | | | | |
| [x]2800 *1* | 0.6 *3* | | | | | |
| 3008 *1* | 2.1 *5* | 3954 | (7/2,9/2,11/2$^-$) | 946 | (9/2$^-$) | |

[†] From revised data Table received from the authors of 2017Sa32, June 5, 2020. Corresponding data in 2017Sa32 are consistent, but rounded to integer values.

[‡] Absolute intensity per 100 decays.

[#] Placement of transition in the level scheme is uncertain.

[x] $\gamma$ ray not placed in level scheme.

## $^{77}$Ni $\beta^-$ decay (158.9 ms) 2017Sa32

### Decay Scheme

Intensities: $I_\gamma$ per 100 parent decays

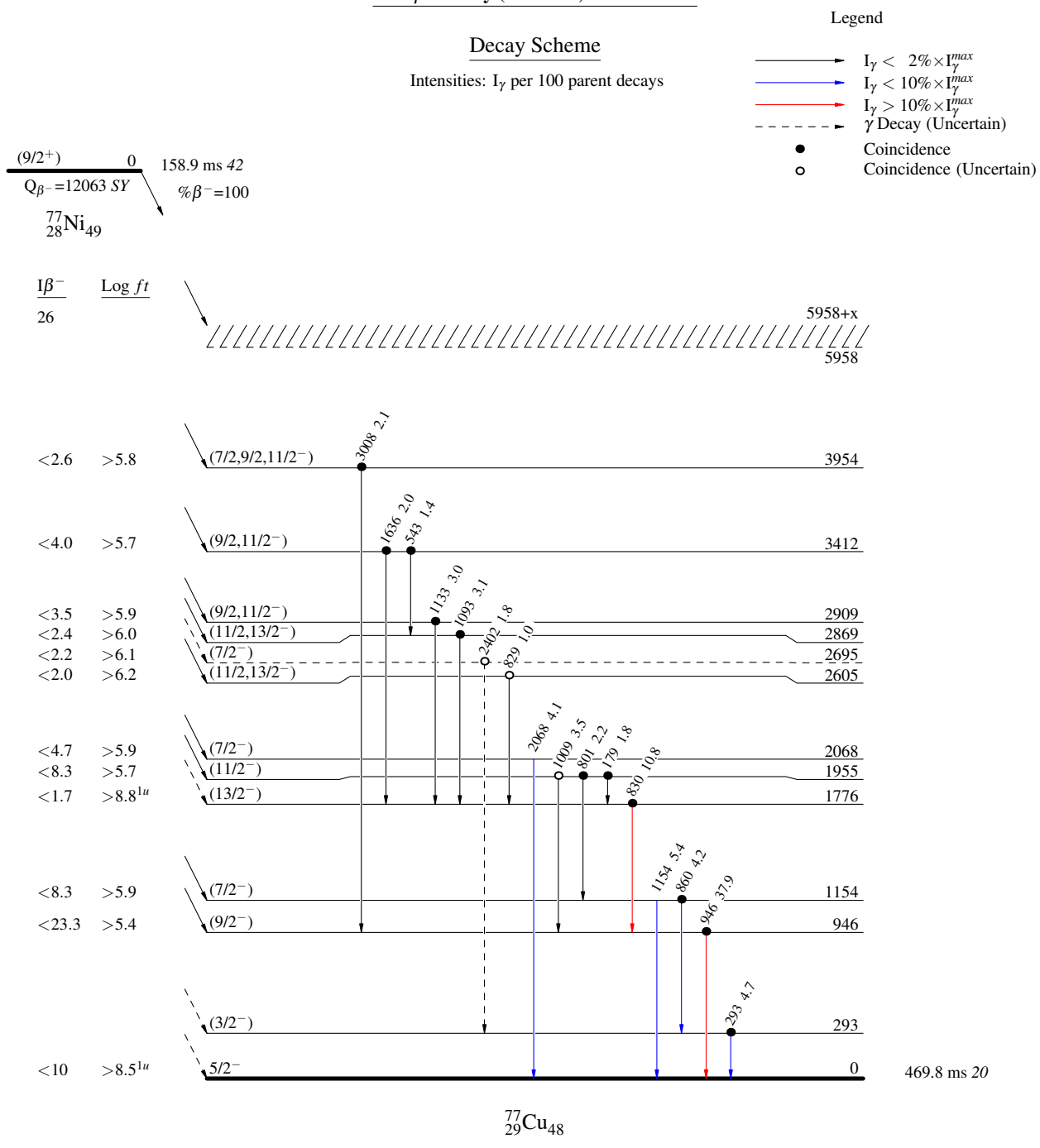


$^{77}_{29}Cu_{48}$